Effect of Chromium Concentration on the Morphology of MAPb $_{1-x}Cr_xBr_3$ Thin Films Synthesized by Spin Coating Process for Solar Cells

D. Soro [1,2*], M. Sidibé [3], B. Marí [2], B. Fofana [1], B. AKA [4], S. Touré [3]
[1]Ecole Normale Superieure (ENS) d'Abidjan, 08 BP 10 Abidjan 08, Côte d'Ivoire
[2]Universitat Politècnica de Vàlencia, Departament de Física Aplicada-IDF, Camí de Vera s/n, Vàlencia, 46022, Spain
[3]Université FHB D'Abidjan-Cocody, Laboratoire d'Energie Solaire, 22 BP 582 Abidjan 22 Côte d'Ivoire
[4] Université Nangui Abrogoua, UFR-SFA, 02 BP 801 Abidjan, Côte d'Ivoire

Abstract – The key materials for the perovskite are compounds with the chemical formula ABX_3 ($A=CH_3NH_3$, B = Pb or Sn, and X = Cl, Br, or I), which have received extensive attention due to their favorable photovoltaic properties. Usually the optical and structural properties of $CH_3NH_3PbBr_3$ can be adjusted by introducing other extrinsic ions such as Cl and I. In this work, instead of replacing Br with I or Cl as usual, we replaced lead with chromium (Cr) which is a transition metal and may have the same oxidation state (+2) as lead. Thin films of $MAPb_{1-x}Cr_xBr_3$ perovskite were produced in a single step from a mixture of MABr, $PbBr_2$ and $(ClO_4)_3Cr$ powders at 45% by weight in a solution of dimethylformamide (DMF). Films were deposited onto ITO-coated glass substrates by spin coating. X-ray diffraction analyses confirmed that these thin-film perovskites crystallize in the cubic phase (Pm-3m) for all composition range $0 \leq x \leq 0.11$. The structural analysis reveals films with (110) and (220) as main peaks and no apparent crystal orientation. SEM analysis shows a morphology with good coverage $MAPb_{1-x}Cr_xBr_3$ showed a high absorbance in the UV–Vis range. The optical band gap was estimated from spectral absorbance measurements. It was found that the onset of the absorption edge for $MAPb_{1-x}Cr_xBr_3$ thin films ranges between 1.60 and 1.80 eV.

Index Terms – MABr; $PbBr_2$; $(ClO_4)_3Cr$, $MAPb_{1-x}Cr_xBr_3$; thin film perovskites, spin coating.

1. INTRODUCTION

In general, the term perovskite defines a kind of crystalline structure composed of three different species (A, B and X) forming the general ABX_3 formula. A and B are two cations of very different sizes. X refers to the anion. In the ideal perovskite structure, the big cations (A^+) are at the corners of a cube. The anions (X^-) are in the middle of each faces; and the small cations (B^{2+}) are in the middle of the octahedral sites formed by the anions.

Organic-inorganic metal halide perovskites have recently shown great potential for application, due to their advantages of low-cost, excellent photoelectric properties and high power conversion efficiency. Their power conversion efficiency (PCE) has increased dramatically from the initial 3.9% in 2009 to current 22.1% in a short span of several years [1–8]. Different fabrication methods have shown that is possible to obtain high quality halide perovskite thin films the film, ranging from vacuum deposition [9], vapor-assisted solution processing [10], atomic layer deposition [11] and solution processing in one and two steps [12–14]. The purpose of this article is to study the role of the chemical substitution of Pb by Cr on the structural, morphological and optical properties of $MAPb_{1-x}Cr_xBr_3$.

2. EXPERIMENTAL PROCEDURE

$MAPb_{1-x}Cr_xBr_3$ were deposited onto the indium tin oxide (ITO)-coated glass substrates by spin coating process. The precursor solutions were prepared by dissolving MABr, $PbBr_2$ and $(ClO_4)_3Cr$ powders at 45% wt Dimethylformamide (DMF) solution. The mixed solutions were stirred for 1 h to ensure the solution homogeneity. The samples were annealed for 1 h at 80 °C and then kept in vacuum to avoid their degradation. Before the deposition, the ITO substrates were cleaned using soapy deionized water and were put in to the ultrasonic bath for 5 min. Then the substrates were thoroughly rinsed with deionized water and different solvents in the following order: acetone and 2-propanol previously warmed in the ultrasonic bath during 5 min each. The crystalline microstructures of the films on ITO substrates were determined using a RIGAKU Ultima IV in the Bragg-Brentano (θ-2θ) configuration employing CuKα radiation (λ = 1.54060 Å). The surface morphology of perovskite films was observed by an environmental scanning electron microscope FESEM (Quanta 200 – FEI) The absorption spectra of perovskite films were carried out at room temperature using spectrometer Ocean Optics HR4000 equipped with a Si-CCD detector and integrating sphere was used to collect specular and diffuse transmittance.

3. RESULTS AND DISCUSSION

3-1. X-Ray analyses

Fig. 1 presents the diffractograms (XRD) of $MAPb_{1-x}CrxBr_3$ for different x values. The $MAPbBr_3$ of perovskite characteristic peaks are located at approximately 15° and 30°

(2Θ), corresponding to planes 110 and 220, respectively. These peaks can be observed for the $MAPbBr_3$ and $MAPb_{1-x}CrxBr_3$.The patterns of all the films display an intense diffraction peaks along (110) and (220) directions. In the case of films where x = 0.7 and 0.11, the patterns have much smaller additional signals in the directions (200), (400) and (330)[15]. The signals are non-existent for x=0.3 and 0.5.

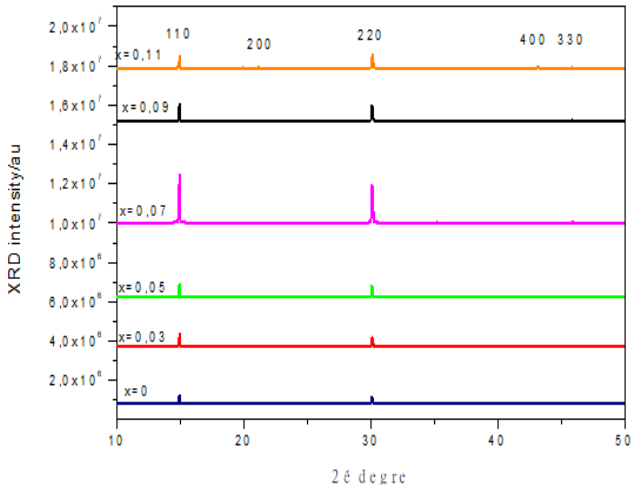

Figure 1: XRD patterns of MAPbBr3 and $MAPb_{1-x}Cr_xBr_3$ deposited by spin coating for all composition range $0 \leq x \leq 0.11$ Reference pattern JCPDS#00-0105 relates to a cubic Pm3m structure.

The samples have diffraction profiles corresponding to those expected for cubic Pm3m. All the synthesized $MAPb_{1-x}Cr_xBr_3$ ($0 \leq x \leq 0.11$) perovskites reported in this paper crystallized in the same cubic phase (space group Pm-3m) independently of the x value The absence of slight displacements of thepeaks towards the upper angles is observed, contrary to what occurs in most cases. These shifts were usually due to the stresses of the crystal lattice caused by interstitial stations. No peaks belonging to impurities and secondary phase were also detected confirming the formation of single-phase crystals.

3-2. Optical properties

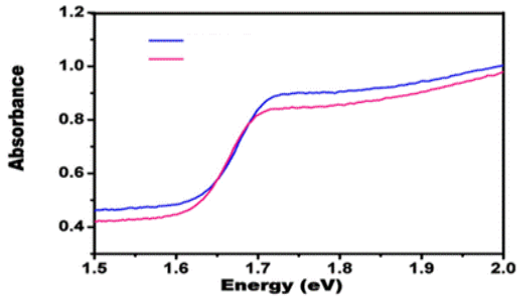

Figure 2: UV–vis absorption spectra of $MAPbBr_3$ and MA $MAPb_{0,93}Cr_{0,7}Br_3$

The organic–inorganic perovskites $MAPb_{1-x}Cr_xBr_3$ were prepared by mixing MABr, $PbBr_2$ and $(ClO_4)_3Cr$ powders in the desired proportions and deposited as thin films onto ITO substrates by spin coating in only one step After analyzing the diffractograms (XRD) of the prerovskites $MAPb_{1-x}Cr_xBr_3$ for different values of x, we chose perovskites $MAPb_{0.93}Cr_{0.07}Br_3$ for the study of its optical properties because of its crystalographic properties. Variation of optical properties of $MAPb_{0.93}Cr_{0.07}Br_3$ and $MAPbBr_3$ perovskite films measured in the UV-visible absorption range was shown in Figure 2. Our results show that changing the molar ratio Pb/Cr in the precursor solution has a significant effect on the morphology, and optical absorption properties of $MAPb_{1-x}Cr_xBr_3$.

Absorbance measurements show that $MAPb_{1-x}Cr_xBr_3$ perovskite films exhibit a very high absorbance. It was found that the onset of the absorption edge for $MAPb_{1-x}Cr_xBr_3$ thin films reaches intermediate values ranging from 1.60 eV to 1.80 eV. These band gap values are very close to the accepted values and this makes the films suitable for optoelectronic devices.

3-3. Microstructure and chemical composition: SEM analysis

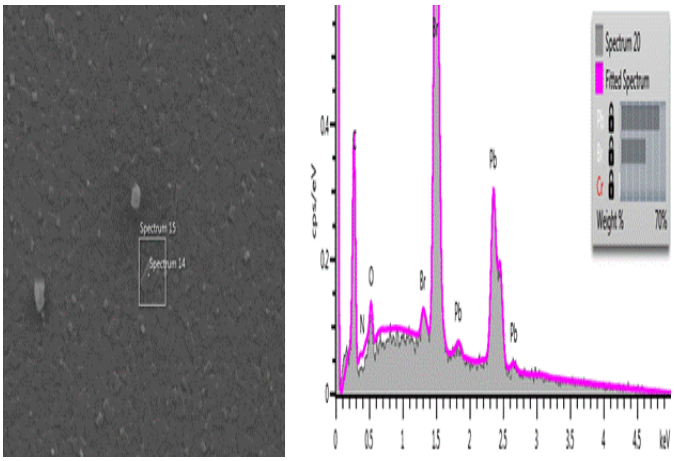

Figure 3: SEM and EDX of $MAPbBr_3$ deposited on ITO substrate using the spin coating process.

The surface morphology of the thin films was observed by SEM image analysis. Figure 3 shows that the chromium-free perovskite film has a homogeneous texture and that the crystalline particles are aggregated into larger crystals. With regard to the thin films of $MAPb_{1-x}Cr_xBr_3$, they appeared to be more or less uniform in all regions, thus covering the substrate well, without the presence of voids, pits or cracks. The small nanoscale grains clearly indicated their surface morphology over the entire substrate, with small particles and some clumps. Figure 4 shows that the thin layers were influenced by the variation of the molar concentration of chromium. Thin films appear less homogeneous. The deposited films seem to be a little rough. Their structure is less uniform with well-defined grain boundaries. We also note a variation in grain size.

Scattered grains are present on the surface of all these films. Energy dispersive X-ray spectrometer (EDX) attached to the SEM was used for the determination of elemental chemical composition. EDX spectra of $MAPbBr_3$ thin films are reported in Fig. 3. The analysis confirmed the presence of Pb and Br elements. No additional peaks attributed to impurities or contaminants, were observed, thereby confirming the purity of the prepared thin films. EDX spectra of $MAPb_{1-x}Cr_xBr_3$, thin films for different x values (Fig. 4, Fig. 5, Fig. 6 Fig. 7) reveals the presence of Pb, Br and Cr elements. The other atomic percentages of Pb and Br of the compound $MaPbBr_3$. In this table, it can be seen that the experimental results are close to the theoretical results. This same observation is made for the atomic percentages of Pb, Br and Cr in the $MAPb_{1-x}Cr_xBr_3$, compound (Table 2). In conclusion, it is found that the compounds $MaPbBr_3$ and $MAPb_{1-x}Cr_xBr_3$, are fairly stoichiometric.

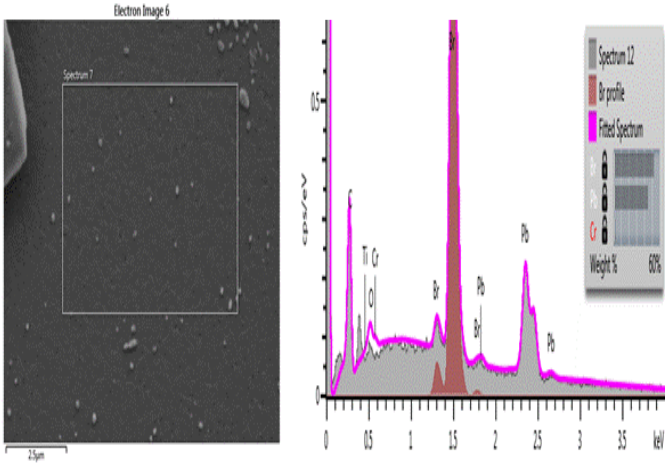

Figure 4: SEM and EDX of $MAPb_{0,97}Cr_{0,03}Br_3$ deposited on ITO substrate using the spin coating process.

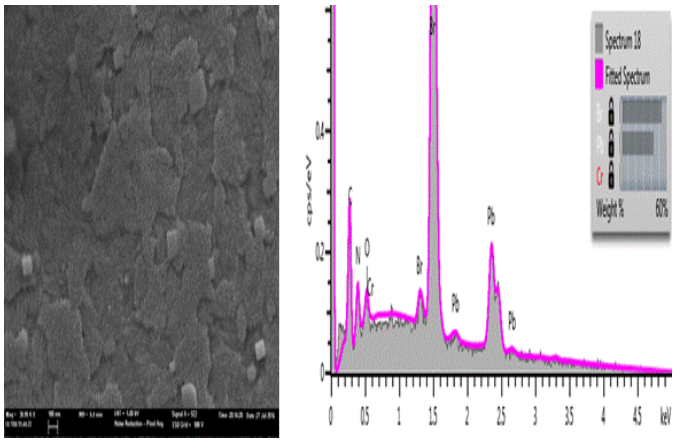

Figure 5: SEM and EDX of $MAPb_{0,93}Cr_{0,07}Br_3$ deposited on ITO substrate using the spin coating process.

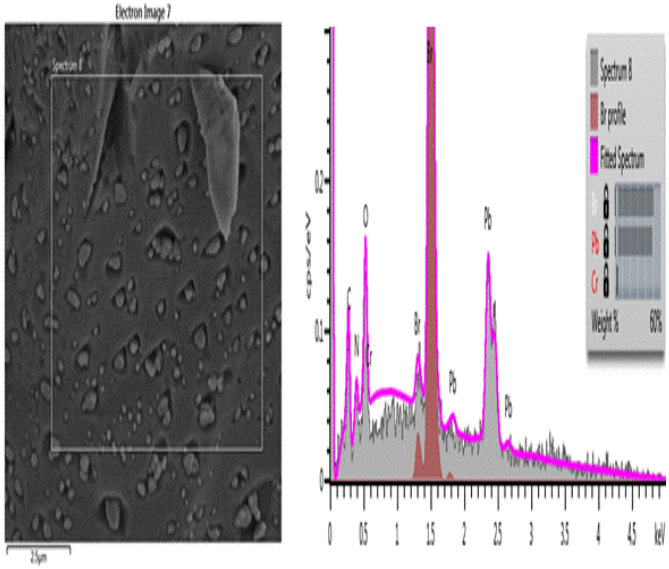

Figure 6: SEM and EDX of $MAPb_{0,91}Cr0,09Br_3$ deposited on ITO substrate using the spin coating process

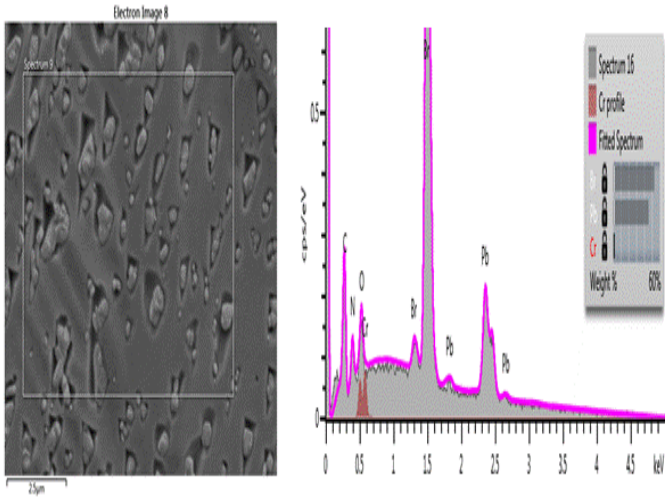

Figure 7: SEM and EDX of $MAPb_{0,89}Cr_{0,11}Br_3$ deposited on ITO substrate using the spin coating process.

Table 1: EDX data of the variation of the atomic percentage between the lead and bromide for MAPbBr3 thin films

Element	Atomic %(theoretical)	Atomic % (experimental)
Br	75.00	74.60
Pb	25	25.40

Table 2 : XRD data of the variation of the atomic percentage between the lead, chromium and bromide for $MAPb_{1-x}Cr_xBr_3$ thin films ($0.03 \leq x \leq 0.11$)

x values	Element	Atomic % (theoretical)	Atomic % (experimental)
0.03	Br	75.00	73.99
	Pb	24.25	24.36
	Cr	0.75	1.65
0.05	Br	75.00	73.88
	Pb	23.75	24.56
	Cr	1.25	1.56
0.07	Br	75.00	73.97
	Pb	23.25	23.40
	Cr	1.75	2.63
0.09	Br	75.00	73.87
	Pb	22.75	22.56
	Cr	2.25	3.57
0.11	Br	75.00	73.89
	Pb	22.25	22.15
	Cr	2.75	3.96

4. CONCLUSION

This work reports the synthesis of $MAPb_{1-x}Cr_xBr_3$ for different x values, deposited on ITO substrate by spin coating. X-Ray diffraction analysis showed that the $MAPbBr_3$ perovskite characteristic peaks were found in the $MAPb_{1-x}Cr_xBr_3$ samples ($0.03 \leq x \leq 0.11$) indicating the Cr incorporation in the $MAPbBr_3$ lattice. The EDX results for all synthesized $MAPb_{1-x}Cr_xBr_3$ samples indicate that MA, Pb, Cr and Br are homogeneously distributed in the perovskite crystal, suggesting that Br; Pb and Cr are uniformly incorporated in the $MAPbBr_3$, and $MAPb_{1-x}Cr_xBr_3$. The estimated band gap (Eg) for samples with a Cr content is between 0 and 11% is between 1.60 and 1.80 eV, respectively, which are very close to the accepted values. This makes $MAPb_{1-x}Cr_xBr_3$ films suitable for optoelectronic devices.

Acknowledgments

This work was supported by Ministerio de Economía y Competitividad (ENE2016-77798-C4-2-R) and Generalitat valenciana (Prometeus 2014/044).

REFERENCES

[1] Kojima, K. Teshima, Y. Shirai, and T. Miyasaka, "Organometal halide perovskites as visible-light sensitizers for photovoltaic cells," Journal of the American Chemical Society, vol. 131, no. 17, pp. 6050–6051, 2009.
[2] H. Zhou, Q. Chen, G. Li et al., "Interface engineering of highly efficient perovskite solar cells," Science, vol. 345, no. 6196, pp. 542–546, 2014.
[3] W. S. Yang, J. H. Noh, N. J. Jeon et al., "High-performance photovoltaic perovskite layers fabricated through intramolecular exchange" Science, vol. 348, no. 6240, pp. 1234–1237, 2015.
[4] N. J. Jeon, J. H. Noh, W. S. Yang et al., "Compositional engineering of perovskite materials for high-performance solar cells," Nature, vol. 517, no. 7535, pp. 476–480, 2015.
[5] Z. Yu and L. Sun, "Recent progress on hole-transporting materials for emerging organometal halide perovskite solar cells," Advanced Energy Materials, vol. 5, no. 12, 2015.
[6] S. Albrecht, M. Saliba, J. P. Baena et al., "Monolithic perovskite/ silicon-heterojunction tandem solar cells processed at low temperature," Energy & Environmental Science, vol. 9, no. 1, pp. 81–88, 2016.
[7] H. S. Jung and N.-G. Park, "Perovskite solar cells: from materials to devices," Small, vol. 11, no. 1, pp. 10–25, 2015.
[8] NREL efficiency chart http://www.nrel.gov/cpv/images/efficiency_chart.jpg, June 2016.
[9] M. Liu, M.B. Johnston, H.J. Snaith, Efficient planar heterojunction perovskite solar cells by vapor deposition, Nature 501 ,pp 395–398, 2013.
[10] Q. Chen, H. Zhou, Z. Hong, S. Luo, H.S. Duan, H.H. Wang, Y. Liu, G. Li, Y. Yang, Planar hetero junction perovskite solar cells via vapor-assisted solution process, J. Am. Chem. Soc. 136 , pp 622–625, 2014.
[11] B.R. Sutherland, S. Hoogland, M.M. Adachi, P. Kanjanaboos, C.T.O. Wong, J.J. McDowell, J. Xu, O. Voznyy, Z. Ning, A.J. Houtepen, E. Sargent, Perovskite thin films via atomic layer deposition, Adv. Mater. 27, pp 53–58, 2015.
[12] J. Burschka, N. Pellet, S.J. Moon, R.H. Baker, P. Gao, M.K. Nazeeruddin, M. Gratzel, Sequential deposition as a route to high-Performance perovskite-Sensitized solar cells, Nature 499, pp 316–319,2013.
[13] M. Lee, J. Teuscher, T. Miyasaka, T.N. Murakami, H.J. Snaith, Efficient hybrid solar cells based on meso-Superstructured organometal halide perovskites, Science 338, pp 643–647, 2012.
[14] J.M. Ball, M.M. Lee, A. Hey, H.J. Snaith, Low-temperature processed meso-superstructured to thin-film perovskite solar cells, Energy Environ. Sci. 6 pp 1739–1743, 2013.
[15] D. Soro, M. Sidibé, W.F. Fassinou, B. Marí, Thierno Sall, B. Fofana, B. AKA, S. Touré, Synthesis of Perfectly Oriented MAPb0,93Cr0,07Br3 Perovskite Crystals for Thin-Film Photovoltaic Applications, Vol. 6, no 6, pp 10170-10176, 2017

Authors

Dr. D. Soro is the corresponding author of this paper and a post graduate Université Nangui Abrogoua, UFR-SFA, 02 BP 801 Abidjan, Côte d'Ivoire. He is a Professor at (ENS) Abidjan, Côte d'Ivoire 08 BP 10 Abidjan 08.

mail: donafologosoro@yahoo.fr

Dr M.Sidibé,Université FHB D'Abidjan-Cocody, 22 BP 582 Abidjan 22, Côte d'Ivoire Laboratory of Solar Energy.

Bernabé Marí Soucase ,professor, Universitat Politècnica de València, Valencia Departament de Física Aplicada-IDF, Camí de Vera s/n, Vàlencia, 46022, Spain.

Aka Boko , professor, Université Nangui Abrogoua, UFR-SFA, 02 BP 801 Abidjan, Côte d'Ivoire, Laboratory IREN UFR-SFA Côte d'Ivoire.

Dr B. Fofana, (ENS) Abidjan, Côte d'Ivoire 08 BP 10 Abidjan 08, Laboratory IREN, Université Nangui Abrogoua, UFR-SFA Côte d'Ivoire.

S.Touré,UniversitéFHB D'Abidjan-Cocody, Laboratory of Solar Energy, 22 BP 582 Abidjan 22, Côte d'Ivoire.